

**In Vitro Resistance of Embryos of *Pinus taeda* to *Cronartium quercuum* f. sp. *fusiforme*:  
Ultrastructure and Histology**

D. J. Gray and H. V. Amerson

Graduate research assistant and visiting assistant professor, respectively, Botany Department, North Carolina State University, Raleigh 27650. (Current address of senior author: Department of Plant and Soil Science, University of Tennessee, Knoxville 37996). Journal Series Paper 8852 of the North Carolina Agricultural Research Service, Raleigh.

This research was supported by several wood products companies via the Southern Forest Research Center at North Carolina State University and by the North Carolina Agricultural Research Service.

We thank C. Lanz, J. Schmidt, and A. Matrone for technical assistance and B. A. Swisher for statistical analyses.

Accepted for publication 17 May 1983.

---

**ABSTRACT**

Gray, D. J., and Amerson, H. V. 1983. In vitro resistance of embryos of *Pinus taeda* to *Cronartium quercuum* f. sp. *fusiforme*: Ultrastructure and histology. *Phytopathology* 73:1492-1499.

Several responses of *Pinus taeda* to infection were noted in vitro as early as 36 hr after inoculation with *Cronartium quercuum* f. sp. *fusiforme* when infected embryos were examined with light and transmission electron microscopy. Incompatible necrosis and apposition formation were among these early host responses. Incompatible necrosis was first characterized by an electron-opaque region that was initiated at the host cytoplasm-vacuole boundary. Concurrently, the host cytoplasm became more densely stained and eventually necrotic. Wall breakdown subsequently occurred. Haustorial necrosis occurred simultaneously or after host cell necrosis with only the haustorial body affected. Also, uninfected cells adjacent to necrotic cells

often became necrotic. Three seed lines of divergent field resistance were used to examine necrosis. Embryos from all three lines exhibited some degree of incompatible necrosis; however, the most resistant line developed the most necrosis thus correlating incompatible necrosis with field resistance. The degree of necrosis appeared similar in all three lines at later sample times. Host wall appositions encountered in penetrated cells of *P. taeda* appeared to simultaneously permit host cell survival and fungal necrosis. Both incompatible necrosis and apposition formation were regarded to be effective host responses to infection.

---

Fusiform rust incited by *Cronartium quercuum* (Berk.) Miyabe ex Shirai f. sp. *fusiforme* is a serious problem for the forest industry in the southeastern USA, inducing woody gall formation in trunks and branches of several susceptible pine species (6). Losses occur

due to seedling death, wind and/or fire damage, and decreased wood quality (6). One of the most widely planted trees in the southeastern USA, loblolly pine (*Pinus taeda* L.), is commonly infected but, fortunately, a measure of additive resistance has enabled foresters to develop several resistant *P. taeda* seed lines. These seed lines were obtained by selections from symptomless trees in nature and were often improved in plant breeding programs (10).

The publication costs of this article were defrayed in part by page charge payment. This article must therefore be hereby marked "advertisement" in accordance with 18 U.S.C. § 1734 solely to indicate this fact.

©1983 The American Phytopathological Society

Plant breeding strategies that are highly successful for developing resistance in annual agricultural species have been hampered for use in perennial *P. taeda*, however, due to the long reproductive cycle of pine trees. Also, to be economically worthwhile, rust resistance must be effective from the seedling stage through marketable age (15–40 yr). This has made rust assessment and breeding a long and complex process in *P. taeda*. Thus, high priority has been placed on developing rust assay systems for early prediction of long-term resistance. Resistance ratings have been obtained as early as 6–7 mo after inoculation with *C. quercuum* at the Resistance Screening Center at Asheville, NC (20); the correlations of seedling reaction to field ratings are  $r = 0.43 - 0.79$  (27). This demonstrates that early screening can predict long-term resistance.

However, the Rust Screening Center system only measures the characteristics of galls. Although the absence of galls is the ultimate expression of resistance, galling is manifested relatively late in the disease cycle, long after responses in gall-free hosts may have operated to confer resistance. Even when gall characteristics are used in resistance evaluation, the gall characters are most likely subsequent expressions of early operative mechanisms. Recognition of these early host responses could lead not only to a better understanding of the disease but also to more efficient management. Individuals or seed lines that possess effective resistance responses could be integrated into breeding programs or propagated with existing tissue culture techniques (24).

The purpose of this study was to identify and describe, via light microscopy and electron microscopy, the variety of host responses seen in embryos of *P. taeda* infected with *C. quercuum* f. sp. *fusiforme* and determine if these responses correlate with field resistance.

## MATERIALS AND METHODS

**Plant source.** This study used three control-pollinated seed lines of widely divergent field resistances (resistance expressed as a numerical performance level [P.L.] obtained from the North Carolina State University Industry Tree Improvement Cooperative to reduce seed source variability. The seed lines were identified by the parental stocks crossed to produce them: 11–23 × 7–34, P.L. 8, susceptible (S); 7–51 × 7–33, P.L. 45, intermediate resistance (I); 7–56 × 7–22, P.L. 77, highly resistant (R). Embryos from these seed lines were aseptically prepared for in vitro inoculation as previously described (2).

**Necrosis studies.** Basidiospore inoculum was prepared by suspending leaves of *Quercus rubra* L. bearing telia in a moist chamber over sterile, glass-distilled, HCl-acidified water, pH 2.2. Basidiospores ejected from telia into the water were concentrated onto a Millipore filter. Spores were resuspended in sterile, glass-distilled water, pH 5.5, and adjusted (using a hemocytometer) to three concentrations: 270,000, 670,000, and 1,570,000 spores per milliliter. Sixty 1- $\mu$ l drops of each concentration were placed on agar, and the basidiospores were counted to verify inoculum concentration. Sterile embryos were inoculated on the hypocotyl with 2- $\mu$ l drops and were incubated in the dark for 24 hr at 22 C. Material was harvested 1.5, 7, and 18 days after inoculation. Only the portion of hypocotyl that had been inoculated was sampled.

Inoculated and uninoculated (control) material was fixed, dehydrated, and epoxy embedded as previously described (9). A minimum of 15 sections, 1  $\mu$ m thick, were obtained and the section from each embryo exhibiting the most pronounced infection was measured. Inoculated specimens with no detectable infection in the 15 sample sections were sectioned completely to verify fungal absence. Transmission electron microscopy was performed on the remaining embedded material of specimens that displayed typical host responses as judged by light microscopy.

The experiment to measure necrosis was designed as a 3 × 3 × 3 factorial experiment with three seed lines, three inoculum levels, and three harvest times as the factors. Each treatment was replicated two to six times, with each replicate consisting of a single embryo. A total of 145 embryos was tested. The parameters measured with light microscopy for necrosis included the percentage

of epidermis exhibiting necrosis (epidermal necrosis), the tissues that became necrotic (tissue necrosis), and the degree of cellular degradation (cellular necrosis). To determine the percentage of epidermal necrosis, we measured the percent of the total hypocotyl circumference on cross sections that was necrotic. Ratings for tissue necrosis were made on a scale of 0–4: no necrosis = 0, hypocotyls with only epidermal necrosis = 1, cortical necrosis = 2, vascular necrosis = 3, and pith necrosis = 4. Cellular necrosis was rated on a scale of 0–2: no necrosis = 0, cells with necrotic cytoplasm = 1, cells with necrotic collapsed walls = 2. Sectioned specimens were randomized in slide boxes prior to grading. Average values of the measurements for these parameters were reported graphically. All data were subjected to an analysis of variance.

**Apposition studies.** Ten embryos from each of the three seed lines were inoculated using nonquantified inoculum as previously described (2). After 7 days, infected and uninfected (control) material was fixed in a 3% phosphate buffered glutaraldehyde solution at 4 C and sectioned at 15  $\mu$ m on a cryostat microtome. Sections were stained and examined for epifluorescence as described by Heath (13). Possible differences in the number of wall appositions between the three lines were subjectively determined by visual inspection.

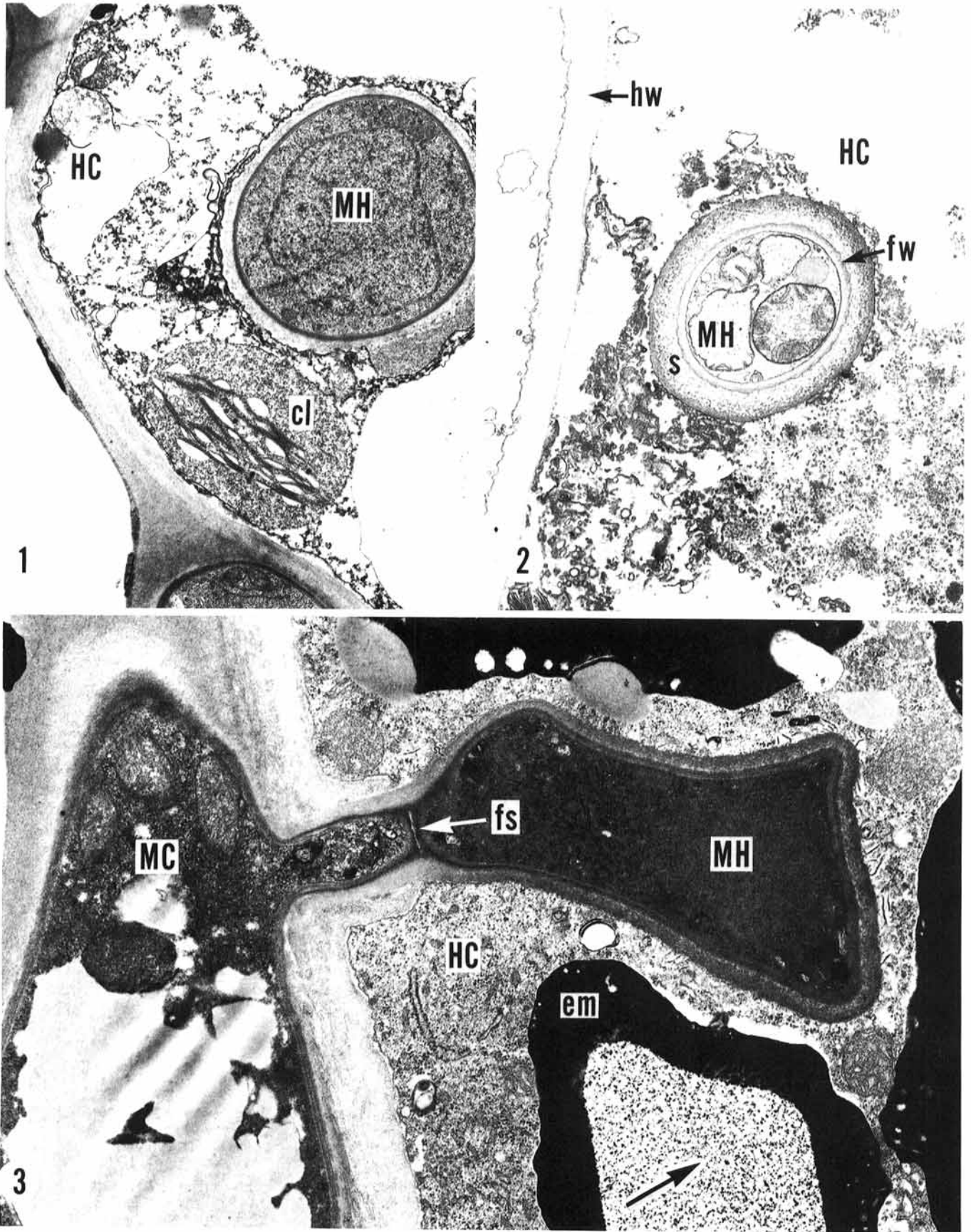
## RESULTS

Infected embryos of *P. taeda* from the susceptible (S), intermediate (I), and resistant (R) seed lines displayed several early developmental traits when examined with light and transmission electron microscopy, including the possession of: abundant lipidlike substances, periderm, hypertrophy accompanied by hyperplasia, cell-tissue necrosis, and wall appositions. However, not all of these traits could be established as host responses to infection. Abundant lipidlike substances were often produced by uninfected plants and therefore may not be a response to disease. Periderms, while not formed by uninoculated plants, were so infrequently encountered (six of 145 plants tested) that they could not be adequately correlated with resistance despite the fact that inoculated embryos with periderm never became infected. Plants exhibiting hypertrophy with hyperplasia, although never infected, were similar in frequency to plants with periderm and so could not be correlated with disease. Only necrosis and deposition of wall appositions were common enough in infected tissues to be confidently designated as host responses that might inhibit fungal penetration and/or colonization. Therefore, these two responses were examined in greater detail.

**Structural types of necrosis.** Two distinct types of necroses, designated compatible (Figs. 1 and 2) and incompatible (Figs. 3 and 4) were noted in hypocotyl tissues from each of three seed lines. Uninfected control embryos infrequently exhibited limited necroses in wounded areas. The ultrastructure of the host-pathogen interface in non-necrotic infected cells has previously been described (7–9).

The compatible necrotic type was difficult to recognize with light microscopy. Ultrastructurally, the compatible type was characterized by a slow breakdown of host organelle structure (Fig. 1) followed by a similar haustorial necrosis (Fig. 2). Both host and fungal cytoplasm became progressively lighter in staining density (Figs. 1 and 2). Adjacent uninfected cells remained intact. Compatible necrosis occurred slowly (perhaps as a normal consequence of senescence) in infected embryo cells and was not, in this study, correlated with resistance of the three seed lines.

The incompatible necrotic type occurred more rapidly and was more easily seen with light microscopy than the compatible type. In the incompatible type, an electron-opaque region was noted in the vacuole along the host tonoplast (Fig. 3); concurrently, densely staining granular material appeared throughout the vacuole. The electron-opaque region enlarged inwardly, apparently occluding the vacuole (Fig. 4, cell with white arrow). Host cytoplasm was initially little changed (Fig. 3), but at later stages of necrosis it became more dense (Fig. 4, cell with black arrow). Host cytoplasm in advanced stages of necrosis was nearly as dense as the electron-opaque material (Fig. 4, cell with white arrow pointing to the



**Figs. 1-3.** Transmission electron micrographs of interfaces between *Cronartium quercuum* f. sp. *fusiforme*-*Pinus taeda* in embryos 7 days after inoculation with 2  $\mu$ l of inoculum suspension containing 670,000 basidiospores per milliliter. **1,** An intermediate stage of a compatible necrotic reaction in a susceptible seed line cortical cell (HC) containing a non-necrotic M-haustorium (MH). Chloroplast (cl),  $\times 10,000$ . **2,** A later stage of the compatible necrotic reaction in a susceptible seed line cortical cell (HC) with a necrotic M-haustorium (MH). Fungal wall (fw), host wall (hw), and sheath(s)  $\times 9,000$ . **3,** An M-haustorium (MH) in a resistant seed line cortical cell (HC) with incompatible necrosis. Electron-opaque material (em) is first visible at the HC cytoplasm-vacuole boundary. Note the densely-staining granular material (arrow) in the vacuole. Fungal septum (fs) and haustorial mother cell (MC),  $\times 19,150$ .



boundary of necrotic cytoplasm and electron-opaque vacuolar region). Membranes of host organelles became less defined in later stages of necrosis (compare Figs. 3 and 4), however, densely-stained membrane fragments often remained (Fig. 4, black arrow). Complete breakdown of the host cell wall eventually occurred.

Haustoria in these incompatible cells did not deteriorate until the electron-opaque regions were easily distinguishable. Necrosis of the haustorial body was characterized initially by an increase in cytoplasmic staining density (Fig. 3) and then by a loss of organelle detail similar to that of the host. However, cytoplasm of the haustorial neck and haustorial mother cell, which was always separated from the haustorial body by a septum (9), was not visibly altered (Fig. 3) in 10 longitudinal profiles examined.

Uninfected cells adjacent to infected, incompatible necrotic cells were also frequently necrotic, creating a densely stained region of tissue around the fungal colony. Plasmodesmata between necrotic cells and adjacent non-necrotic cells (Fig. 4) sometimes contained electron-opaque material characteristic of incompatible necrosis.

**Development of incompatible necrotic tissues.** Typical necrotic

areas were obvious in the epidermis of the hypocotyl of *P. taeda* within 36 hr after inoculation in all three seed lines but were most prevalent in the R line. Necrosis spread from the epidermis into the cortical and vascular tissues, eventually reaching the pith in some specimens. Fungal hyphae were not always visible in these necrotic regions by light microscopy due to the densely-staining nature of the necrotic material. However, electron microscopy confirmed hyphal presence in selected specimens. Occasionally hyphae were seen in advance of necrotic regions.

**Correlation of incompatible necrosis with resistance.** In the R seed line epidermal necrosis was more than twice as great as in the S and I lines when data from all times and inoculum levels were pooled (Fig. 5). However, examination of the data over time (Fig. 6) revealed that the significantly greater mean for epidermal necrosis in Fig. 5 for the R line was due to rapid necrosis occurring at 1.5 and 7 days (Fig. 6). Epidermal necrosis of R increased little between the 7th and 18th days. However, by the 18th day, necrosis of the I line increased to a level nearly equal to that of the R line (Fig. 6).

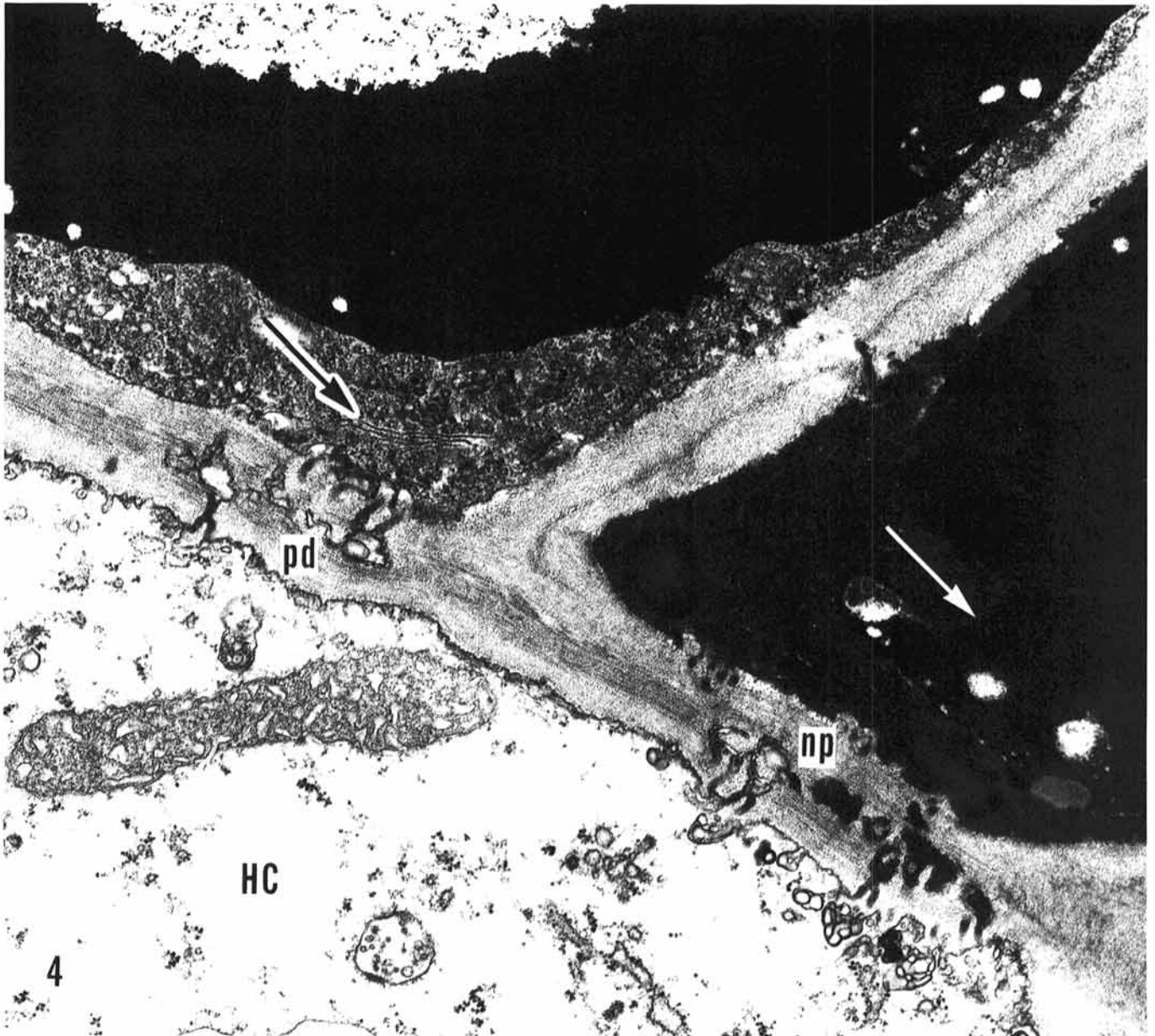


**Fig. 4.** A transmission electron micrograph of a necrotic embryo of *Pinus taeda* from the intermediate seed line 7 days after inoculation with  $2 \mu\text{l}$  of inoculum suspension containing 670,000 basidiospores of *Cronartium quercuum* f. sp. *fusiforme* (incompatible type necrosis). Three cortical cells depicting stages of necrosis, ranging from nonnecrotic cortical cell (HC) to a partially necrotic cell (black arrow) to a highly necrotic cell (white arrow). Although HC is not necrotic, it appears abnormal due to dilated cytoplasm. Non-necrotic plasmodesmata (pd) and necrotic plasmodesmata (np).  $\times 20,900$ .

A seed line  $\times$  inoculum level interaction was apparent for epidermal necrosis. Only the R seed line reacted preferentially to an inoculum level of 670,000 spores per milliliter, showing significantly more epidermal necrosis with this inoculum than at the lower and higher levels (Fig. 7).

The development of tissue necrosis in the hypocotyl was the second means for distinguishing resistance (Fig. 8). It was apparent, however, that assessment would only be valid at certain sample times. This is illustrated in Fig. 8 where, at 36 hr, all three lines exhibited primarily necrosis of the epidermis but not deeper tissues. However, at 7 days the resistant line possessed significantly more necrotic tissues. At 18 days necrotic tissues in R and I lines were equivalent and more extensive than in the S line (Fig. 8). It appears that necrosis was initially confined to superficial layers in all three lines, but at a relatively early stage, R seed line tissues became necrotic at a greater rate. However, as was seen in Fig. 6 for percent epidermal necrosis, between 7 and 18 days the rate that

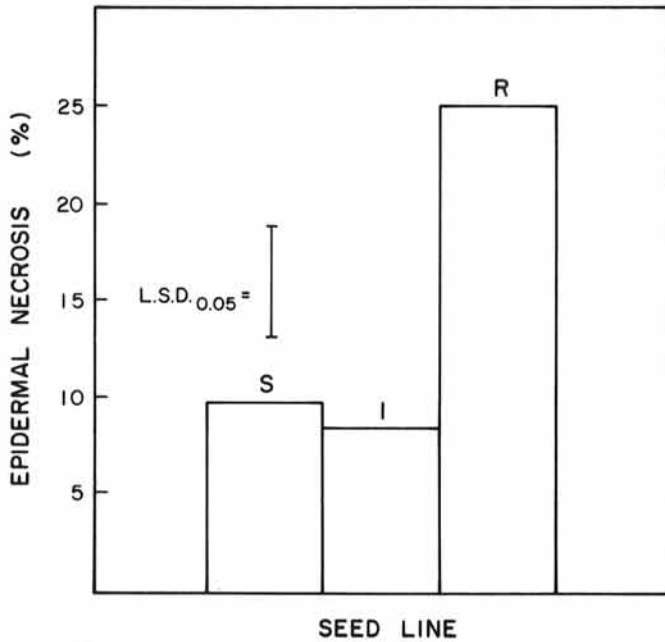


Fig. 5. Percentage of incompatible epidermal necrosis in embryos of three seed lines of *Pinus taeda* inoculated in vitro with basidiospores of *Cronartium quercuum* f. sp. *fusiforme*. Each bar of the graph represents pooled data from all sample times (1.5, 7, and 18 days) at three inoculum concentrations (540, 1,340, and 3,140 spores per embryo).

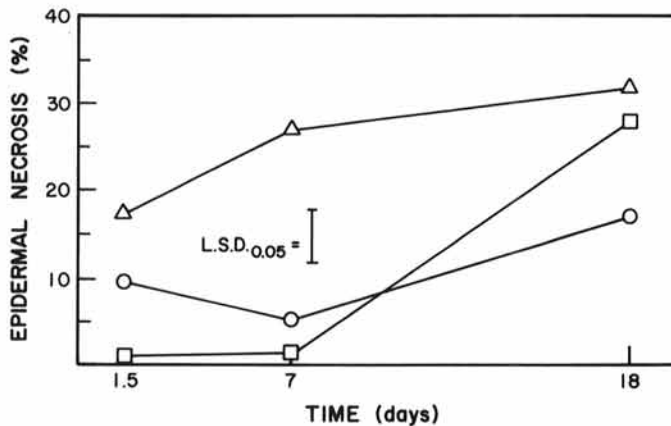


Fig. 6. Percentage of incompatible epidermal necrosis at designated times in embryos of three seed lines of *Pinus taeda* inoculated in vitro with basidiospores of *Cronartium quercuum* f. sp. *fusiforme*. Each datum point reflects three pooled inoculum levels ( $2 \mu\text{l}$  per embryo from inocula containing either  $27 \times 10^4$ ,  $67 \times 10^4$ , or  $157 \times 10^4$  basidiospores per milliliter). Resistant line ( $\Delta$ ), intermediate line ( $\square$ ), susceptible line ( $\circ$ ).

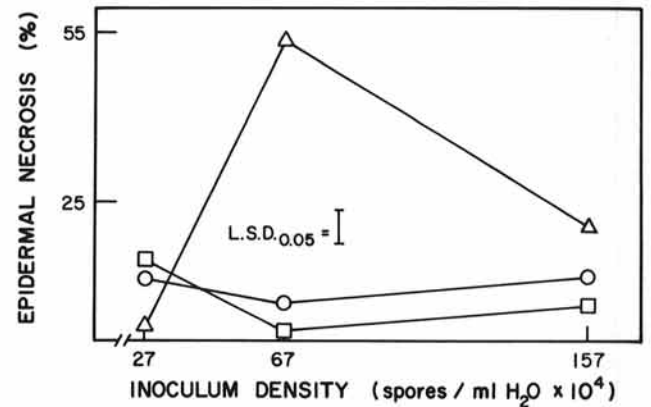


Fig. 7. Percentage of incompatible epidermal necrosis in embryos of three seed lines of *Pinus taeda* inoculated in vitro with basidiospores of *Cronartium quercuum* f. sp. *fusiforme* at three concentrations. The inoculum was  $2 \mu\text{l}$  per embryo containing either  $27 \times 10^4$ ,  $67 \times 10^4$ , or  $157 \times 10^4$  basidiospores per milliliter. Each datum point represents specimens evaluated 1.5, 7, and 18 days after inoculation. Resistant line ( $\Delta$ ), intermediate line ( $\square$ ), susceptible line ( $\circ$ ).

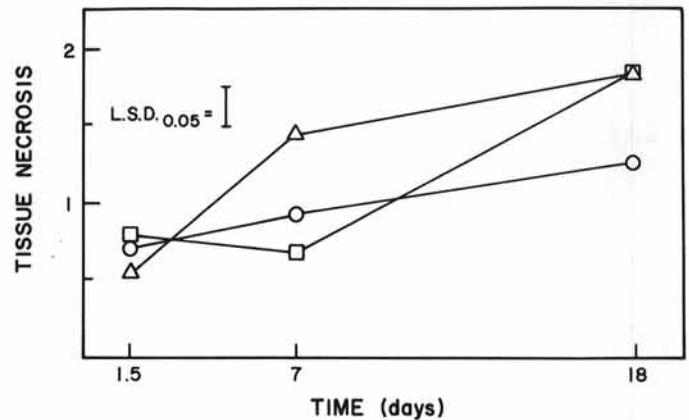


Fig. 8. A comparison of incompatible tissue necrosis at designated times in embryos of three seed lines of *Pinus taeda* inoculated in vitro with basidiospores of *Cronartium quercuum* f. sp. *fusiforme*. Necrosis was rated as: no necrosis = 0, epidermal necrosis = 1, cortical necrosis = 2, vascular necrosis = 3, and pith necrosis = 4. Values are expressed as averages. Each datum point reflects three pooled inoculum levels ( $2 \mu\text{l}$  per embryo from inocula containing either  $27 \times 10^4$ ,  $67 \times 10^4$ , or  $157 \times 10^4$  basidiospores per milliliter). Resistant line ( $\Delta$ ), intermediate line ( $\square$ ), susceptible line ( $\circ$ ).

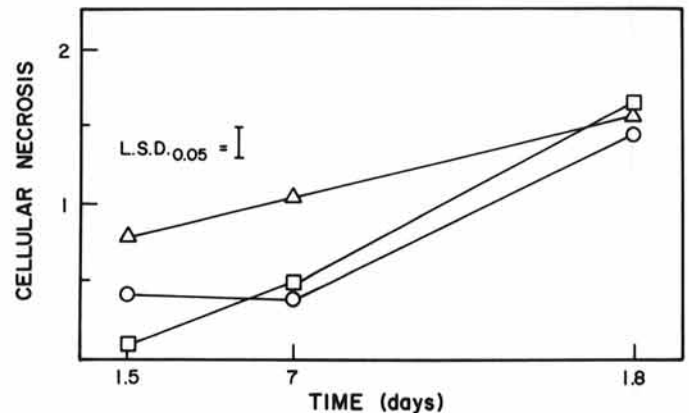
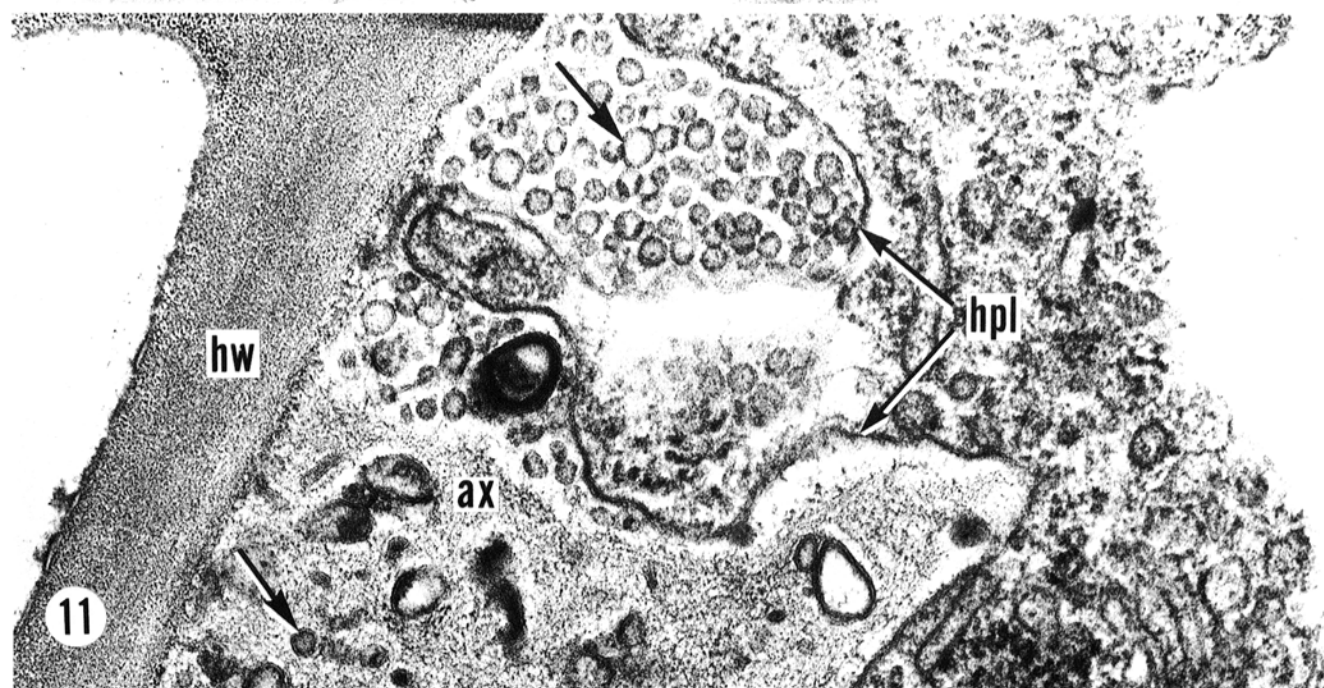
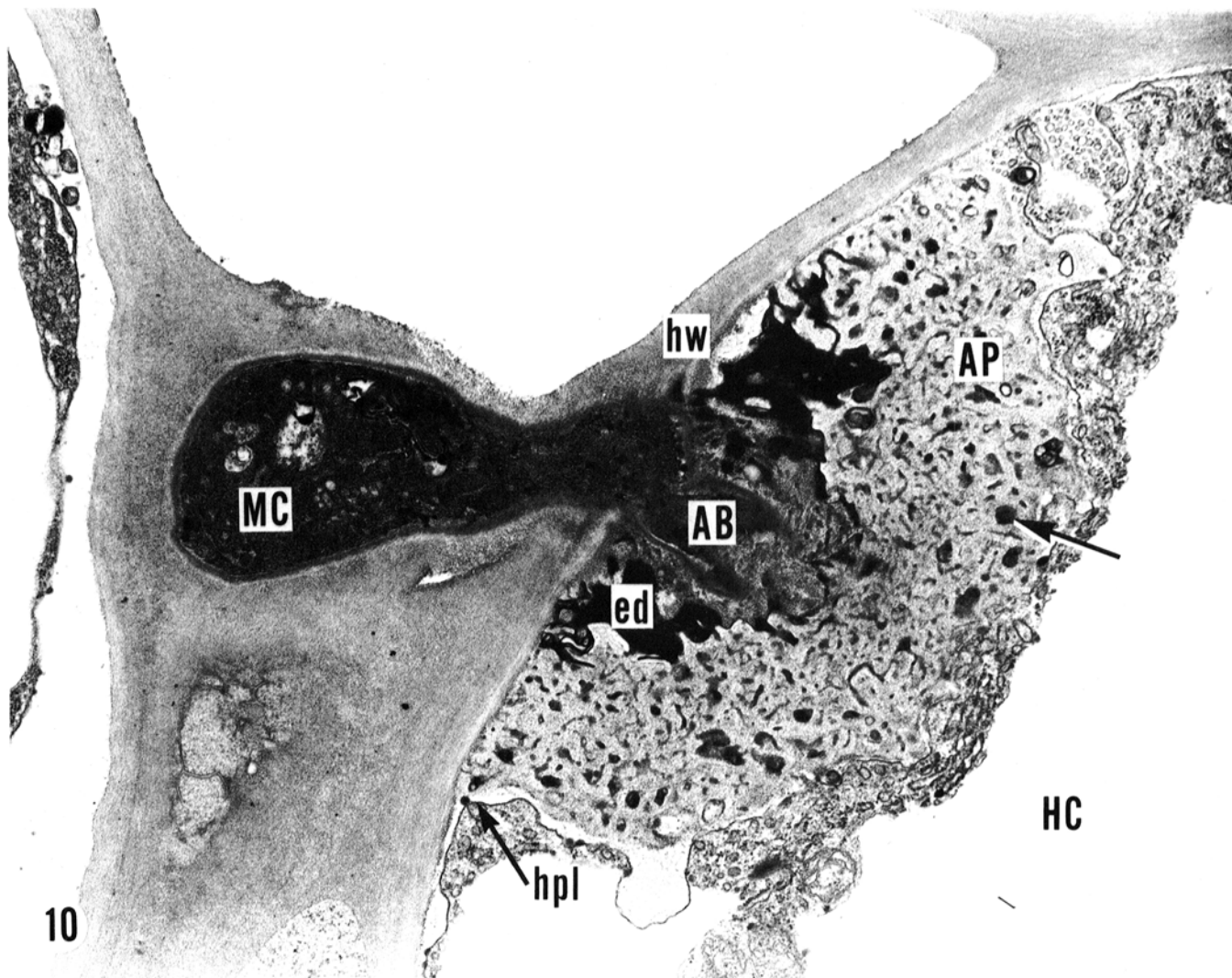


Fig. 9. A comparison of incompatible cellular necrosis at designated times in embryos of three *Pinus taeda* seed lines inoculated in vitro with *Cronartium quercuum* f. sp. *fusiforme* basidiospores. Necrosis was rated as: no necrosis = 0, cytoplasmic necrosis = 1, and cellular collapse = 2. Values are expressed as averages. Each datum point reflects three pooled inoculum levels ( $2 \mu\text{l}$  per embryo from inocula containing either  $27 \times 10^4$ ,  $67 \times 10^4$ , or  $157 \times 10^4$  basidiospores per milliliter). Resistant line ( $\Delta$ ), intermediate line ( $\square$ ), and susceptible line ( $\circ$ ).



**Figs. 10–11.** Transmission electron micrographs of interfaces between *Cronartium quercuum* f. sp. *fusiforme* and *Pinus taeda* in an embryo of the intermediately resistant host seed line inoculated in vitro with a nonquantified number of basidiospores. **10**, Penetrated cortical cell (HC) with apposition (AP). Both extracellular haustorial mother cell (MC) and intracellular portions of the aborted fungal element (AB) are necrotic. Arrow indicates electron-dense vesicle. Electron-dense material (ed), host plasmalemma (hpl), and host wall (hw),  $\times 16,710$ . **11**, Higher magnification of a part of Fig. 10 detailing numerous membrane-bound electron-lucent vesicles (upper arrow) between the host plasmalemma (hpl) and host cell wall (hw). Lower arrow indicates an intact electron-lucent vesicle embedded in the apposition matrix (ax),  $\times 60,370$ .



deeper tissues became necrotic slowed in the R line but increased in the I line so that eventually R and I embryos appeared similar. The S line developed necrosis at a much slower rate so that final necrosis was the least (Fig. 8).

The severity of cell necrosis provided a third measure that correlated with resistance. Cellular necrosis was most advanced in the R line at early infection stages (36 hr and 7 days) but became equivalent in I and S lines at later times (Fig. 9). This is an indication that cellular necrosis occurred early in the R line and that cells of the I and S lines, although becoming equally as necrotic, did so more slowly.

In general, measurement of these three parameters: epidermal necrosis, tissue necrosis, and cellular necrosis demonstrated that the R line differed from either I or S lines in the severity of incompatible necrosis. Although specimens from each line could be found that exhibited either incompatible or compatible reactions, the R line developed significantly more incompatible necrosis. The I and S lines usually did not statistically differ from each other (Figs. 5, 6, 8, 9).

**Structure of wall appositions.** Wall appositions, which could be routinely found with fluorescence microscopy (Fig. 12), were irregularly observed with electron microscopy in all three lines. Appositions, when formed, appeared to provide an effective cellular barrier to fungal invasion, allowing attacked cells to survive by walling off and causing necrosis of the intruding fungal element (Fig. 10). Appositions occurred between the host cell wall and plasmalemma and were of heterogenous origin, being composed of an amorphous matrix containing membrane-bound, electron-dense vesicles interspersed throughout (Figs. 10, 11). Other electron-dense material, possibly identical to that in the vesicles, was accumulated around the aborted fungal element (Fig. 10). The host cytoplasm bordering the apposition was highly vesiculate, and numerous small membrane-bound, electron-lucent vesicles were apparent in an outer portion of the apposition (Figs. 10 and 11). These vesicles also appeared to be embedded in the electron-lucent apposition matrix (Fig. 11). Thus, the matrix material in this region contained two types of inclusions: large, densely-stained membranous vesicles, and smaller membrane bound vesicles filled with electron-lucent material (Fig. 11).

## DISCUSSION

A diversity of early developmental traits was observed in this study. Although, for several reasons, not all could be related to disease resistance with statistical analysis, these traits are interesting nevertheless. For example, embryos exhibiting two traits, early

periderm formation or hyperplasia with hypertrophy, were never infected; this perhaps corresponds to the Type I immune reaction reported by Miller et al (23). Therefore, further study of such early developmental traits is warranted in the search for disease resistance.

**Necrosis.** The electron-opaque material that accompanied the incompatible type necrosis was first visualized ultrastructurally in this work, but a similar material was reported in previous light microscope studies of infected *P. elliotii* var. *elliotii* (18,23,26). Miller et al (23) described heavily-stained necrotic cells containing haustoria "encrusted," presumably, by the same material which in thin sections appeared electron-opaque. We did not determine the composition of this material, but others (26) have demonstrated that tannins or tannin precursors are abundant in fusiform rust-infected tissues. In addition, Jewell and Spiers (18) reported an increase in "tanninization" in cells from necrotic zones similar to those noted in this study. Therefore, the evidence points to a phenolic origin for the electron-opaque material.

Necrosis was not observed in the haustorial neck and intercellular mycelium, but necrosis of the haustorial body was always either concurrent with or preceded by host necrosis in fusiform rust-infected embryos of *P. taeda*. Ultrastructural studies of other host-rust infections have revealed great differences in the sequence of cell and haustorium necrosis. Workers have reported instances similar to this study where host cell death usually preceded haustorial necrosis (11,19,22,28). Conversely, others have demonstrated haustorial necrosis followed by host cell necrosis (25), and in some instances haustoria were unaffected while host cells became necrotic (1). Furthermore, this and another study (23) of fusiform rust have demonstrated that the necrotic response can be propagated through uninfected cells in advance of the invading colony. It is difficult to assess the importance of individual cell necrosis in inhibiting fungal colonization based on such varied data. It may be that host cell necrosis in response to haustorial invasion does not directly limit spread of the fungal mycelium. Rather, haustorial invasion may induce host cell necrosis and this, in turn, may serve to "trigger" the death of adjacent cells connected by plasmodesmata (Fig. 4). The fungal colony would be inhibited indirectly by necrosis of the penetrated cell when adjacent uninfected cells quickly died and became unsuitable for infection.

Each of the three parameters measured for necrotic host responses demonstrated primarily one trend: the R seed line was capable of developing cell and tissue necrosis at greater rates early in the infection process than either the I or S lines. This shows a correlation of rapid necrosis in the R line with resistance and points to the importance of selecting the proper sample time for accurate disease assessment. The apparent decrease in the rate of necrosis in the R line at later infection stages was possibly artifactual, however, since available tissue for necrosis could have been exhausted earlier due to the rapidity of the response. The I and S seed lines were similar in that tissues of each were not as necrotic at early infection stages (Figs. 6 and 9). However, only the I line exhibited a significant increase in the rate of tissue necrosis at later stages (Fig. 8), suggesting that the I line is less resistant than the R line but more resistant than the S due to a delayed necrotic response. This would be similar to the necrotic response in the mesothetic reaction studied by Higgins (16) for wheat resistance to *Puccinia graminis* Pers. f. sp. *tritici*.

**Wall appositions.** The formation of wall appositions has not been previously demonstrated in fusiform rust, but the preponderance of studies reporting such appositions in other rust-host interactions (1,5,12,13,19) makes this discovery unsurprising. Electron-lucent material identical to that noted in wall appositions is deposited in lesser, apparently non-effective, amounts as collars encasing haustorial necks of the monokaryotic phase (7,9) and portions of intracellular infection structures (7,8) in embryo epidermal cells of *P. taeda*. Studies of the dikaryotic infection stage in *Quercus rubra* L. demonstrate similar appositions encasing necrotic dikaryotic haustoria (7). The electron-lucent portions of collars and appositions are thought to be at least partially composed of callose (4).

The structure of wall appositions formed by cells of *P. taeda* in

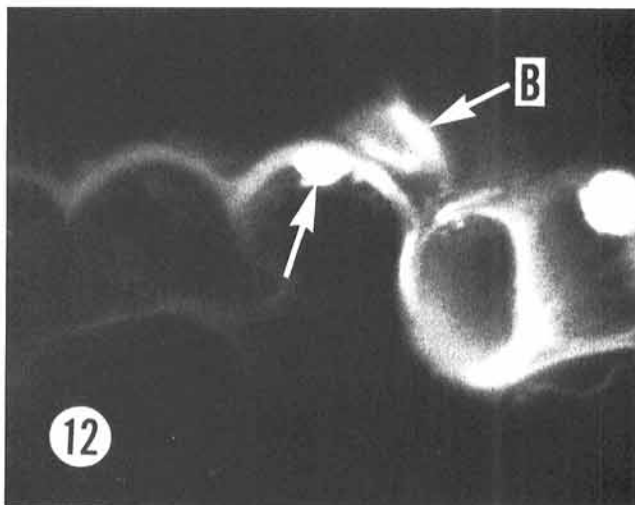


Fig. 12. Fluorescence microscopy of interfaces between *Cronartium quercuum* f. sp. *fusiforme* and *Pinus taeda* in an embryo of the susceptible line inoculated in vitro with a nonquantified number of basidiospores. Wall apposition (arrow) in epidermal cell. Basidiospore (B) on hypocotyl surface.  $\times 1,860$ .

response to fusiform rust invasion was similar to appositions formed as a result of other rust-host interactions. Littlefield and Heath (21), summarizing previous studies, stated that callose-like material is probably deposited from vesicles of uncertain cytoplasmic origin which fuse with the host plasmalemma, liberating their contents between the plasmalemma and host or fungal wall. However, questions remain as to how the small membrane-bound, electron-lucent material is deposited between the host plasmalemma and cell wall as seen in the present study. Our data suggest that either this material becomes membrane-bound as a result of exocytosis from the host plasmalemma or that these membrane-bound vesicles are formed in the cytoplasm and then deposited against the host cell wall when breaks occur in the highly active plasmalemma. That the appearance and the extent of callose-like substances can be influenced by glutaraldehyde fixation (17) also raises the possibility that these vesicles may be artifactual.

The production of appositions as an effective barrier to infection is probably of little consequence when considering internal cells and tissues, since not all cells in a sample formed appositions in response to infection. However, the potential of resistance due to apposition formation deserves more attention with regard to fusiform rust disease, because the fungus must penetrate through an epidermal cell. Genotypes selected for their ability to form abundant epidermal cell appositions (Fig. 12) could preclude internal colonization.

**In vitro resistance.** This study has shown that tissue cultured embryos inoculated with rust basidiospores in vitro can display a wide variety of host responses and that some of these responses (ie, rapid necrosis) can be correlated with disease resistance (see Figs. 5-9). Thus, the opportunity for an in vitro resistance assay exists, and efforts to establish such an assay for the fusiform rust disease of loblolly pine are underway in our laboratory. The assay that we are now developing depends on the in vitro inoculation of tissue cultured materials followed by microscopic assessment in free-hand sections. This assay will offer advantages in rapidity, host uniformity via tissue culture, and precise environmental regulation. However, researchers should also recognize that potential disadvantages do exist, especially in those assays dependent upon actual fungal infection rather than fungal-derived toxins (3). In the present study, inoculum level and assessment time were critical for necrosis evaluation, and others (14,15) have demonstrated that changes in culture conditions can alter host responses. Despite the obvious need for caution, assays of tissue culture materials offer promising alternatives to long-term whole plant assays.

#### LITERATURE CITED

1. Abu-Zinada, A. A. H., Cobb, A., and Boulter, D. 1975. An electron-microscopic study of the effects of parasite interaction between *Vicia fabia* L. and *Uromyces fabae*. *Physiol. Plant Pathol.* 5:113-118.
2. Amerson, H. V., and Mott, R. L. 1978. Technique for axenic production and application of *Cronartium fusiforme* basidiospores. *Phytopathology* 68:673-675.
3. Amerson, H. V., and Mott, R. L. 1982. Phytopathology and tissue culture alliances. Pages 208-230 in: J. M. Bonga and D. J. Durzan, eds. *Tissue Culture in Forestry*. Martinus Nijhoff Publ. The Hague, Netherlands.
4. Chong, J., and Harder, D. E. 1982. Ultrastructure of haustorium development in *Puccinia coronata avenae*: Some host responses. *Phytopathology* 72:1527-1533.
5. Coffey, M. D. 1976. Flax rust resistance involving the *K* gene: An ultrastructural survey. *Can. J. Bot.* 54:1443-1457.
6. Dinus, R. J., and Schmidt, R. A. 1977. Management of fusiform rust in southern pines. *Symp. Proc., Univ. Fla., Gainesville*. 167 pp.
7. Gray, D. J. 1982. Ultrastructure and histology of the fusiform rust fungus. Ph.D. thesis. North Carolina State University, Raleigh. 122 pp.
8. Gray, D. J., Amerson, H. V., and Van Dyke, C. G. 1983. Ultrastructure of the infection and early colonization of *Pinus taeda* by *Cronartium quercuum* formae specialis *fusiforme*. *Mycologia* 75:117-130.
9. Gray, D. J., Amerson, H. V., and Van Dyke, C. G. 1982. An ultrastructural comparison of monokaryotic and dikaryotic haustoria formed by the fusiform rust fungus *Cronartium quercuum* f. sp. *fusiforme*. *Can. J. Bot.* 60:2914-2922.
10. Hanna, H., and Draper, L., Jr. 1977. Fusiform rust management strategies in practice: Seed source manipulation. Pages 134-144 in: R. J. Dinus and R. A. Schmidt, eds. *Management of Fusiform Rust in Southern Pines*. *Symp. Proc., Univ. Fla., Gainesville*. 167 pp.
11. Harder, D. E., Samborski, D. J., Rohringer, R., Rimmer, S. R., Kim, W. K., and Chong, J. 1980. Electron microscopy of susceptible and resistant near isogenic (*Sr6/sr6*) lines of wheat infected by *Puccinia graminis tritici*. III. Ultrastructure of incompatible interactions. *Can. J. Bot.* 57:2626-2634.
12. Heath, M. C. 1972. Ultrastructure of host and nonhost reactions to cowpea rust. *Phytopathology* 62:27-38.
13. Heath, M. C. 1977. A comparative study of nonhost interactions with rust fungi. *Physiol. Plant Pathol.* 10:73-88.
14. Helgeson, J. P., Haberlach, G. T., and Upper, C. D. 1976. A dominant gene conferring disease resistance to tobacco plants is expressed in tissue cultures. *Phytopathology* 66:91-96.
15. Helgeson, J. P., Kemp, J. D., Haberlach, G. T., and Maxwell, D. P. 1972. A tissue culture system for studying disease resistance: The black shank disease in tobacco callus cultures. *Phytopathology* 62:1439-1443.
16. Higgins, V. J. 1981. Histological comparison of compatible, mesothetic, and incompatible reactions between *Puccinia graminis tritici* and wheat. *Can. J. Bot.* 59:161-165.
17. Hughes, J. E., and Gunning, B. E. S. 1980. Glutaraldehyde-induced deposition of callose. *Can. J. Bot.* 58:250-258.
18. Jewell, F. F., and Speirs, D. C. 1975. Histopathology of one- and two-year-old resisted infections by *Cronartium fusiforme* in slash pine. *Phytopathology* 66:741-748.
19. Jonsson, A., Holmvall, M., and Walles, B. 1978. Ultrastructural studies of resistance mechanisms in *Pinus sylvestris* L. against *Melampsora pinitorqua* (Brunn) Rostr. *Stud. For. Suec.* 145:1-28.
20. Laird, P. P., and Phelps, W. R. 1975. A rapid method for mass screening of loblolly and slash pine seedlings for resistance to fusiform rust. *Plant Dis. Rep.* 59:238-242.
21. Littlefield, L. J., and Heath, M. C. 1979. *Ultrastructure of Rust Fungi*. Academic Press, New York. 277 pp.
22. Mares, D. J. 1979. Microscopic study of the development of yellow rust (*Puccinia striiformis*) in a wheat cultivar showing adult plant resistance. *Physiol. Plant Pathol.* 15:289-296.
23. Miller, T., Cowling, E. B., Powers, H. R., Jr., and Blalock, T. E. 1976. Types of resistance and compatibility in slash pine seedlings infected by *Cronartium fusiforme*. *Phytopathology* 66:1229-1235.
24. Mott, R. L., and Amerson, H. V. 1980. A tissue culture process for the clonal production of loblolly pine plantlets. *North Carolina Agric. Res. Serv., Tech. Bull.* 271, 14 pp.
25. Prusky, D., Dinooor, A., and Jacoby, B. 1980. The sequence of death of haustoria and host cells during the hypersensitive reaction of oat to crown rust. *Physiol. Plant Pathol.* 17:33-40.
26. Walkinshaw, C. H. 1978. Cell necrosis and fungal content in fusiform-rust-infected loblolly, longleaf, and slash pine seedlings. *Phytopathology* 68:1705-1710.
27. Walkinshaw, C. H., Dell, T. R., and Hubbard, S. D. 1980. Predicted field performance of slash pine families from inoculated greenhouse seedlings. U.S. Dep. Agric. For. Serv., Res. Pap. 50-160 pp.
28. Zimmer, D. E. 1970. Fine structure of *Puccinia carthami* and the ultrastructural nature of exclusionary seedling-rust resistance of safflower. *Phytopathology* 60:1157-1163.